

# ROCK-II mediates colon cancer invasion via regulation of MMP-2 and MMP-13 at the site of invadopodia as revealed by multiphoton imaging

Ramana Vishnubhotla<sup>1,\*</sup>, Shan Sun<sup>1,\*</sup>, Jameela Huq<sup>1</sup>, Marinka Bulic<sup>2</sup>, Anil Ramesh<sup>2</sup>, Grace Guzman<sup>3</sup>, Michael Cho<sup>1</sup> and Sarah C Glover<sup>1,2,4</sup>

The ROCK-II isoform of Rho's downstream effector, Rho kinase, has been linked with greater invasion and metastasis in solid tumors. We have previously shown that ROCK-II is overexpressed at the advancing edge of colon cancers. The mechanism whereby ROCK-II contributes invasion, particularly in the setting of colon cancer, remains to be elucidated fully. To better understand its contribution, we evaluated ROCK-II expression in both non-malignant (NCM460 and IEC-6) and malignant (Caco-2 E, SW620, and HCT-116) intestinal epithelial cell lines grown in type I collagen scaffolds. Using multiphoton microscopy, we observed that ROCK-II localized to the actin cytoskeleton in non-malignant cells but localized to the cell periphery as focal collections with an absence of adjacent collagen in all colon cancer cell lines. By transmission electron microscopy, these collections corresponded with finger-like projections previously described as invadopodia. Immunogold staining with cortactin, matrix metalloprotease (MMP)-2, -9, and -13 confirmed that these were indeed invadopodia. To further link ROCK-II to colon cancer invasion, we treated non-malignant and malignant intestinal epithelial cell lines with ROCK-II siRNA and evaluated depth of invasion, proliferation, and MMP-2, -9, and -13 activities. The most striking effect was seen in the highly tumorigenic cell lines, SW620 and HCT-116, wherein ROCK-II knockdown resulted in a two-fold or more reduction in invasion. This reduction in invasion was not due to a decrease in cell proliferation, as a significant reduction in proliferation was only observed in the two non-malignant intestinal cell lines. Finally, both MMP-2 and -13 activities were significantly decreased in all colon cancer cell lines. Taken together, these data suggest for the first time that ROCK-II is a critical mediator of colon cancer cell invasion through its modulation of MMP-2 and -13 at the site of invadopodia but regulates proliferation in non-malignant intestinal cells.

*Laboratory Investigation* (2007) **87**, 1149–1158; doi:10.1038/labinvest.3700674; published online 17 September 2007

**KEYWORDS:** ROCK-II; invadopodia; colon cancer; matrix metalloprotease; extracellular matrix; proliferation

The contribution of the Rho-like members of the Rho GTPase family and their downstream effectors to cancer progression and invasion remains controversial.<sup>1–3</sup> In the case of Rho A, it has been shown to both promote and retard epithelial-to-mesenchymal transition (EMT).<sup>4–8</sup> Rho B has been shown to be proapoptotic and may actually be important in retarding EMT, whereas Rho C has been linked with greater metastasis through its ability to disrupt adherens junctions. Central to the action of these proteins is their downstream effector, Rho kinase (ROCK).<sup>9</sup>

Unlike its upstream activators, ROCK's role in cancer is less controversial. ROCK has two major isoforms designated

ROCK-I and ROCK-II. ROCK-II has been linked with greater invasion in several solid tumors.<sup>1,2</sup> Studies performed in colon cancer cell lines have shown that when ROCK-II is overexpressed, it promotes tumor growth by reducing the association between tumor cells. This reduction in cell–cell adhesion promotes movement and allows for migration of endothelial cells into the tumor, a process that may lead to the formation of new vascular channels.<sup>10</sup> Furthermore, when ROCK-II is activated in *in vitro* colon cancer cell models it produced greater instability at the sites of adherens junction formation.<sup>9</sup> While these studies have provided important information about the contribution of ROCK-II to

<sup>1</sup>Department of Bioengineering, University of Illinois at Chicago, Chicago, IL, USA; <sup>2</sup>Department of Medicine, University of Illinois at Chicago, Chicago, IL, USA; <sup>3</sup>Department of Pathology, University of Illinois at Chicago, Chicago, IL, USA and <sup>4</sup>Department of Medicine, Jesse Brown VA Medical Center, Chicago, IL, USA  
Correspondence: Dr SC Glover, DO, Department of Medicine, University of Illinois at Chicago, 840 South Wood Street, MC 716, Chicago, IL 60612, USA.  
E-mail: sarahg@uic.edu

\*These authors contributed equally to this work.

Received 01 February 2007; revised 08 August 2007; accepted 10 August 2007

the disruption of adherens junctions in colon cancer, they do not fully answer the question of how it contributes to invasion in colon cancer.

In colon cancer, activity at the invasion front or advancing edge of the tumor has been demonstrated to be most predictive of further invasion and metastasis.<sup>11–13</sup> Since the major extracellular matrix component near the advancing edge of colon cancers is type I collagen,<sup>14</sup> we examined the contribution of ROCK-II to colon cancer cell invasion at the tumor advancing edge using three-dimensional type I collagen scaffolds and multiphoton microscopy in non-malignant and malignant intestinal epithelial cell lines. In doing so, we found that ROCK-II played a dynamic role in colon cancer invasion through its action on matrix metalloprotease (MMP)-2 and -13 at the site of invadopodia, but acted as a regulator of proliferation in non-malignant intestinal epithelial cell lines.

## MATERIALS AND METHODS

### Reagents and Supplies

All cell culture reagents, excluding M3F base (Incell Inc.), Opti-MEM (Invitrogen, Carlsbad, CA, USA), low carbonate DMEM (ATCC, Manassas, VA, USA), and FBS (Gemini Bio-Products), were obtained from Mediatech Inc. (Herndon, VA, USA). Bovine insulin was purchased from Sigma-Aldrich (St Louis, MO, USA). Caco-2 E cells, a subclone of Caco-2 BBE cells, were a generous gift from Dr Jerrold Turner at the University of Chicago. IEC-6 (ATCC# CRL-1592), HCT-116 (ATCC# CCL-247), and SW620 cells (ATCC# CCL-227) were purchased from ATCC. NCM460 cells were obtained under license agreement from Incell Inc. Cells were maintained in dishware from BD Falcon (Lincoln Park, NJ, USA). Type I rat tail collagen was purchased from BD Bioscience. Mammalian protease inhibitor cocktail was purchased from Sigma-Aldrich. Cell extracts were equalized using the BCA Protein Assay kit from Pierce (Rockford, IL, USA). Antibodies recognizing ROCK, MMPs, cortactin, and lamin-A as well as HRP conjugated secondary antibodies were from Santa Cruz (Camarillo, CA, USA). Florescent staining was performed with FITC- and TRITC-labeled anti-goat IgG from Sigma-Aldrich. All other florescent stains were obtained from Invitrogen. Transmission electron microscopy (TEM) grade supplies and immunogold-labeled streptavidin were purchased from EMS and LX112 epoxy resin from LADD Research (Wiliston, VT, USA). Antigen retrieval solution, serum-free protein block, and antibody diluent were purchased from DakoCytomation (Carpinteria, CA, USA). Western blot analysis was performed using the ECL Plus detection system from GE Healthcare (Piscataway, NJ, USA) and PVDF transfer membranes from Millipore. Proliferation was observed using 'Vybrant<sup>®</sup> MTT Cell Proliferation Assay kit' from Invitrogen. siRNA experiments were conducted using an siCONTROL scrambled sequence from Dharmacon (Lafayette, CO, USA). All other siRNA reagents were from Santa Cruz including ROCK II siRNA (sc-29474). Matrix

Metalloprotease Assay kits were purchased from R&D Systems (Minneapolis, MN, USA). All other supplies were molecular biology grade and were from Fisher (Pittsburg, PA, USA).

### Cell Culture

NCM 460 cells were cultured in M3F Base supplemented with 10% fetal bovine serum and were incubated at 37°C in a 5% CO<sub>2</sub> atmosphere. IEC-6 cells were cultured in low carbonate DMEM with 0.1 units/ml bovine insulin supplemented with 10% fetal bovine serum and incubated in a 5% CO<sub>2</sub> atmosphere. Caco-2 E cells were cultured in DMEM/F-12 50/50 1× with L-glutamine and 15 mM HEPES supplemented with 10% fetal bovine serum and were incubated at 37°C in a 5% CO<sub>2</sub> atmosphere. SW620 cells were cultured in Leibovitz's L-15 medium 1× with L-glutamine supplemented with 10% fetal bovine serum and were incubated at 37°C in a 1% CO<sub>2</sub> atmosphere. HCT-116 cells were cultured in McCoy's 5A supplemented with 10% fetal bovine serum and were incubated at 37°C in a 5% CO<sub>2</sub> atmosphere.

### Western Blotting

Each cell line was grown to 70% confluence in a standard tissue culture flask. Cells were then lysed using primary lysis buffer (50 mM HEPES, 150 mM sodium chloride, 1.5 mM magnesium chloride, 100 mM sodium fluoride, 10 mM sodium pyrophosphate) containing 1:50 dilution of protease inhibitor cocktail. Protein concentrations were determined using the BCA reagent with 40 µg of each extract electrophoresed per lane on a 7.5% polyacrylamide gel under denaturing and reducing conditions. The resolved proteins were electrophoretically transferred to PVDF membranes. Immunoreactive bands were visualized using either ROCK-I at 4 µg/ml, ROCK-II at 2 µg/ml, or B-actin at 1 µg/ml followed by horseradish peroxidase conjugated bovine anti-goat IgG and the ECL Plus detection system.

### Preparation of 3-D Scaffolds

Three-dimensional cell cultures were performed as described previously.<sup>15</sup> Briefly, 3 mg/ml type I collagen in 0.1 M acetic acid was mixed with equal portions of 0.1 M NaOH, 0.7% sodium bicarbonate, and Hank's Balanced Salt Solution 10× for a final type I collagen concentration of 1.5 mg/ml. The pH was adjusted to 7.4 and serum-free culture media were added so that it made up 30% of the mixture. Predetermined amounts of this mixture were placed on glass supports and allowed to gelatinize. A low density of the colonic epithelial cell line of interest ( $2 \times 10^5$  cells/cm<sup>2</sup>) was then be plated on top of the gel. Gels were incubated at 37°C for 1 h at which time an additional 2 ml of appropriate media was added.

### Immunocytochemistry and Multiphoton Microscopy

Cell-containing collagen scaffolds were cultured for up to 48 h at 37°C at the appropriate CO<sub>2</sub> level. Scaffolds were then washed with phosphate-buffered saline (PBS), fixed

overnight with 10% neutral buffered formalin, and then permeabilized with tris-buffered saline with 0.05% Tween-20 (TBST) for 5 min. After this, the scaffolds were blocked for 20 min with serum-free protein block and then incubated overnight at 4°C with desired primary antibody. Scaffolds were then washed with TBST, incubated with a fluorescently labeled secondary antibody for 30 min, and finally stained with phalloxin and DAPI prior to imaging.

Collagen fibrillar structure and seeded cells were imaged by a laser scanning multiphoton confocal microscope with  $\times 60$  oil objective (NA = 1.40). DAPI was visualized by using multiphoton laser excitation at 700 nm and emission at 450 nm, for which the femtosecond laser beam (80 MHz, 0.5 mW) pumped from a mode-locked titanium/Sapphire laser (MaiTai, Spectra-Physics Inc., CA, USA), was coupled with visible laser (Bio-Rad, UK) into an inverted laser scanning confocal microscope (Nikon TE200-U, Japan). Reflection signals from the collagen fibers were excited and acquired at a wavelength of 488 nm.

### Transmission Electron Microscopy

Cells were plated on top of type I collagen scaffolds as above and allowed to invade over a 24-h period. At the end of this time, media were removed; scaffolds were washed with sterile PBS, and then fixed with 3% glutaraldehyde in 0.1 M sodium cacodylate buffer. Post fixation, the cell-containing scaffolds were treated with 1% osmium tetrachloride and dehydrated using graded ethanol. The samples were then infiltrated with and embedded in epoxy resin, LX112.83 nm sections were made using a Leica Ultracut II, and placed on 150-mesh nickel grids. Sections were then steamed for 20 min in a citrate-based antigen retrieval solution. When cool, the sections were then blocked using serum-free protein block. Each section was then probed for the primary antibody of interest for 2 h followed by the appropriate biotinylated secondary antibody for 1 h. Finally, sections were incubated with streptavidin-gold (6 nm gold particle) at 1:20 dilution in TBS, pH 7.6 for 1 h, and then counterstained with 5% uranyl acetate and Reynold's lead citrate. Sections were viewed and images were obtained using a JEOL JEM-1220 transmission electron microscope. Primary antibody concentrations used were as follows: cortactin, MMP-2, -9, and -13 were used at 10  $\mu\text{g}/\text{ml}$ , and ROCK-II was used at 20  $\mu\text{g}/\text{ml}$ .

### Proliferation Assay

Cell proliferation was determined using a standard MTT Assay kit. All components used were free of phenol red, since it could potentially interfere with the accuracy of the assay. To do this, the media were removed from each chamber and the gels were washed with PBS. Hundred microliters of fresh media and 20  $\mu\text{l}$  of dye ((3-(4,5-dimethylthiazol-2-yl)-2,5-diphenyltetrazolium bromide) in PBS were added to each chamber. The gels were incubated at 37°C for 4 h. After 4 h, 50  $\mu\text{l}$  from each chamber was added to 100  $\mu\text{l}$  of dimethylsulfoxide in a small vial and incubated for 15 min.

Absorbance readings were taken at 550 nm for each sample to determine the cell proliferation values.

### ROCK-II siRNA

Cells were grown to confluence and then disaggregated and plated at  $2 \times 10^5$  cells per  $\text{cm}^2$ . Plates will be incubated until at least 70% confluent in antibiotic-free media. When desired confluence was reached, growth media were removed; cells were washed with transfection medium, and then transfected with the 5  $\mu\text{l}$  of 20  $\mu\text{M}$  siRNA of interest per well according to the manufacturer's instructions. A scrambled sequence was used as a control. Transfection efficiency was determined by western blot 24 h post transfection.

### MMP Activity

MMP-2, -9, and -13 activities were determined using a quantitative sandwich enzyme immunoassay technique. Briefly, a monoclonal antibody specific for each MMP was pre-coated onto a microplate. Standards and samples were placed into the wells, and the MMP of interest was bound by the immobilized antibody. After washing away unbound substances, an enzyme-linked polyclonal antibody specific for each MMP was added to the wells. Following a wash to remove unbound antibody-enzyme reagent, a substrate solution was added to the wells and color developed in proportion to the amount of total the MMP being analyzed (pro and/or active) bound in the initial step. Following addition of a stop solution, absorbance was measured at 450 nm using a standard microplate reader. This method has been validated against zymography by R&D Systems.

### Statistics

Data were analyzed using Student's *t*-distribution using average values and the associated standard deviation. A comparative *P*-value of less than 0.05 was considered significant.

### RESULTS

In our previous histological studies of colon cancer specimens, we have observed that ROCK-II, not ROCK-I, was upregulated at the tumor-advancing edge.<sup>3</sup> Our findings coupled with data from the solid tumor literature demonstrating that ROCK-II overexpression correlated with greater invasion and metastasis<sup>1,2</sup> led us to investigate whether or not ROCK-II played a role in colon cancer invasion in an *in vitro* model.

### ROCK-II Expression Not Significantly Impacted by Intestinal Cell Type

To begin, it was necessary to establish a model system to evaluate ROCK-II's behavior. To do this, we first evaluated ROCK-I and -II expressions in non-malignant (NCM460 and IEC-6) and malignant (Caco-2 E, SW620, and HCT-116) intestinal epithelial cell lines. NCM460 cells are a non-malignant human colonic epithelial cell line<sup>16</sup> and IEC-6 cells

are a non-malignant rat small intestinal cell line. While IEC-6 cells are not colonic in origin, we used them in addition to NCM460 cells so that we could validate our observations about ROCK-II in at least two non-malignant cell lines. Caco-2 E cells are a non-tumorigenic colon cancer cell line derived from a tumor of unknown differentiation, which have a villous appearance and well-organized tight junctions on TEM. In contrast, SW620 cells are highly aggressive colon cancer cell line originally derived from a lymph node metastasis.<sup>17</sup> They have been shown to produce liver metastases in nude mice.<sup>18</sup> HCT-116 cells are a poorly differentiated colon cancer cell line, which have been shown to produce local lymph node metastases in a nude mouse model.<sup>18</sup>

Western blots were performed on extracts from each of these cell lines to assess their expression of ROCK-I and -II (Figure 1). While all five intestinal cell lines expressed ROCK-I, there was significantly less ROCK-I expressed by HCT-116 cells. Similarly, ROCK-II was expressed by all five intestinal cell lines but appeared as multiple bands. The least amount of fragmentation of ROCK-II was noted with HCT-116 cells and was expressed as two distinct bands at 160 and 130 kDa. Others have shown that this can occur and is due to fragmentation of ROCK-II by proteases such as Granzyme B.<sup>19</sup> This same paper showed that the cleaved product that appears as a band at 130 kDa is active.

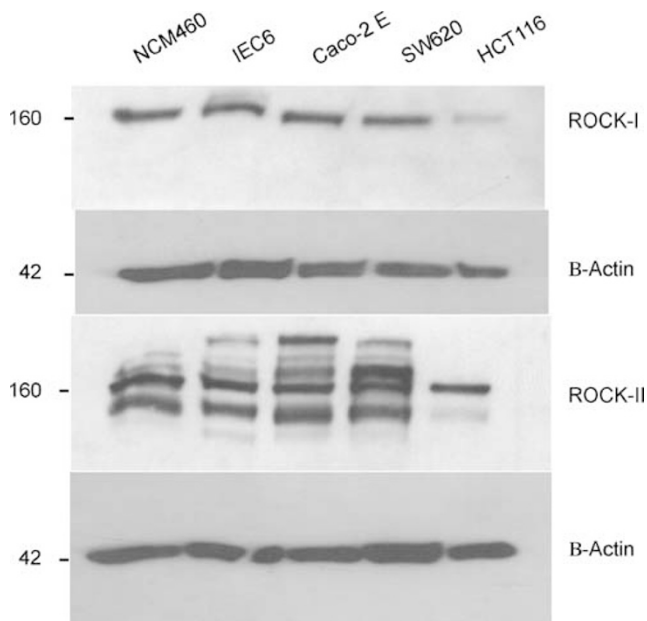


**Figure 1** ROCK-I and -II are expressed in non-malignant and malignant intestinal cell lines. All five cell lines express ROCK-I, but HCT-116 cells have significantly lower ROCK-I expression than the other four cell lines. All five cell lines express ROCK-II. The least amount of fragmentation of ROCK-II was seen in HCT-116 cells in which two bands were visualized at 160 and 130 kDa respectively. B-actin was used as a loading control. This experiment was repeated in triplicate.

### ROCK-II Localization Differs between Non-Malignant Intestinal Cells and Colon Cancer Cells

Because intracellular localization often provides insight into function, we next evaluated ROCK-II expression of each colonic epithelial cell line in type I collagen scaffolds. Type I collagen was chosen because it is a predominant extracellular matrix protein in the advancing edge of colon cancers.<sup>14</sup> The scaffolds were created to be fairly stiff so as to have a rigidity more reminiscent of the tumor microenvironment at the advancing edge of a tumor. As described in the Materials and methods section, cells were seeded on top of these gels and allowed to invade and remodel over a 24-h period. Cell-containing scaffolds were then probed with antibodies to ROCK-II, appropriate counterstains, and imaged using a multiphoton microscope.

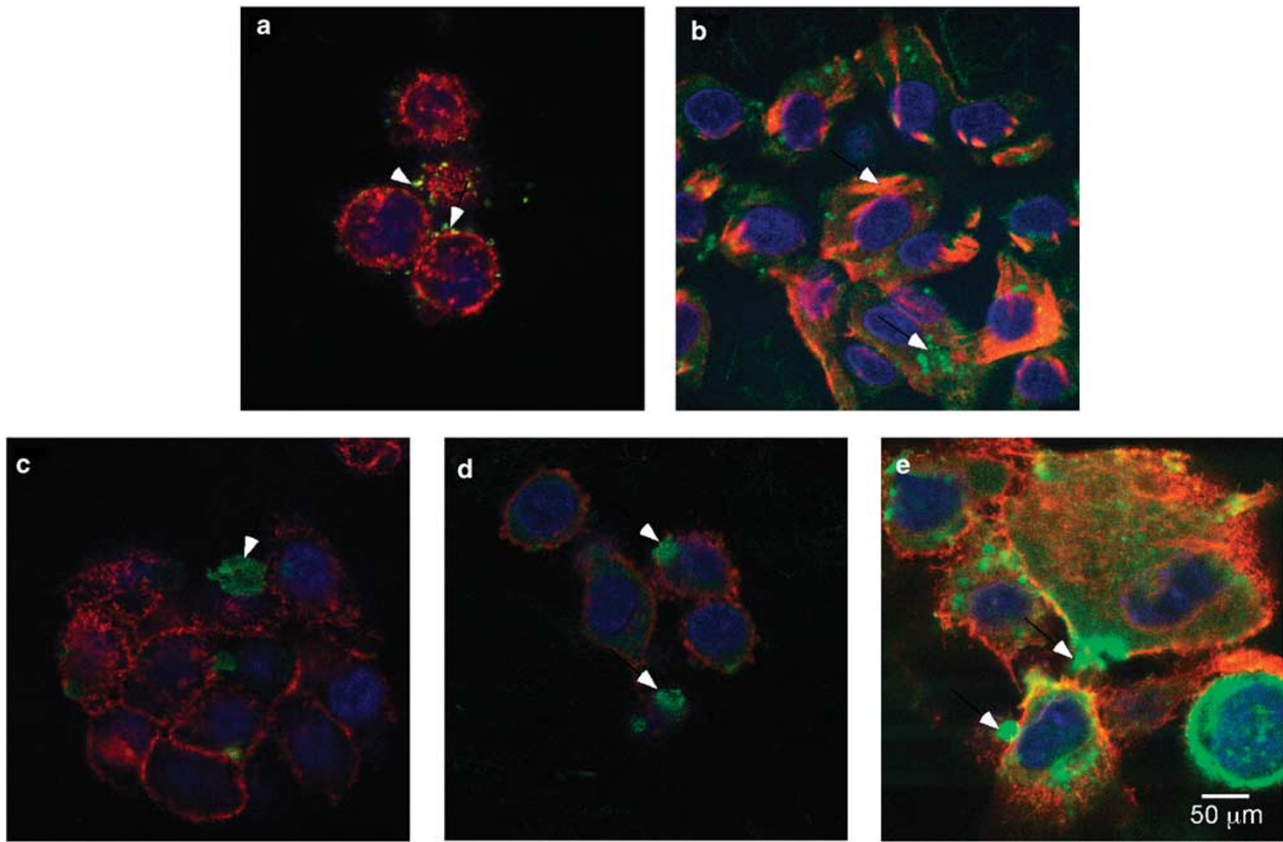
As shown in Figure 2, ROCK-II colocalized with the actin cytoskeleton for both the non-malignant intestinal cell lines (Figure 2a and b). However, ROCK-II localized to peripheral projections in the three malignant cell lines (Figure 2c–e). These peripheral ROCK-II collections did not colocalize with actin in either of the three malignant colonic epithelial cell lines. The significance of this finding becomes more apparent in Figure 3.

Figure 3 shows multiphoton images each of the five intestinal cell lines probed with ROCK-II (red), stained with DAPI to identify nuclei (blue), and imaged to capture the autofluorescence of the collagen (green). Similar to Figure 2, ROCK-II appears as punctate structures in both NCM460 and IEC-6 cells. There is no significant collagen degradation adjacent to these structures. In contrast, significant collagen degradation is noted adjacent to the peripheral ROCK-II-positive collections in each of the colon cancer cell lines (Figure 3c–e). This finding led us to consider the possibility that these ROCK-II collections may actually be associated with a matrix degrading structures such as invadopodia.

Invadopodia are podosome-like structures capable of focal matrix degradation.<sup>20–24</sup> They were first identified in breast cancer cell lines and have classically been seen in an ‘invadopodia’ assay wherein cells are seeded on fibronectin-coated gelatin and the number of matrix degrading extensions is noted.

### ROCK-II Localizes to Invadopodia

To confirm that these structures were invadopodia, we plated each cell line at equal densities on type I collagen scaffolds and processed them for TEM as described in the Materials and methods section. In non-malignant NCM460 and IEC-6 cells, no structures representing invadopodia were noted (data not shown). In Caco2-E, SW620, and HCT-116 cells, structures resembling invadopodia were identified. Representative images of invadopodia in SW620 cells probed with antibodies to cortactin (Figure 4b), ROCK-II (Figure 4c), MMP-2 (Figure 4d), MMP-9, (Figure 4e), and MMP-13 (Figure 4f) are show in Figure 4.



**Figure 2** ROCK-II localizes to the actin cytoskeleton in non-malignant intestinal cell lines, but localizes at the cell periphery in malignant cell lines. Non-malignant (NCM 460 (a) and IEC-6 (b)) and malignant intestinal cell lines (Caco-2 E (c), SW620 (d), and HCT-116 (e)) were seeded onto type I collagen scaffolds and allowed to invade over a 24-h period. Scaffolds were then fixed and stained for ROCK II (green), actin (red), and nuclei (blue). Non-malignant cell lines show ROCK-II colocalizing with the actin cytoskeleton. Malignant cell lines show heavy ROCK-II expression localizes to the cell periphery. Negative controls for each cell line were probed with a goat IgG and no staining was seen (data not shown). Bar = 50  $\mu$ m.

Cortactin staining was evaluated because this protein has been shown to be a marker of invadopodia.<sup>25–27</sup> As shown in Figure 4b, cortactin staining is noted at the base of the invadopodia structure. ROCK-II localized to the tips of these structures as well as to discrete collections in the cytoplasm of the cell.

Since invadopodia degrade the matrix, we next confirmed that these projections possessed matrix-degrading enzymes. To do this, we probed TEM sections of SW620 cells for several MMPs that have been previously localized to invadopodia, specifically MMP-2, MMP-9, and MMP-13. MMP-2 has been previously localized to invadopodia<sup>28</sup> and action on MMP-2 by MMP-1 has been shown to lead to clustering of its active form at the site of invadopodia.<sup>29,30</sup> MMP-9 has been localized to invadopodia in highly invasive breast cancer cells.<sup>31</sup> MMP-13 has been previously shown to localized to invadopodia in several gastric cancer cell lines.<sup>32</sup> Evaluation of each of these MMPs revealed localization to the sites of invadopodia. While all the three MMPs were present, MMP-2 and -13 were the most robust and clustered at the tips of the invadopodia along with ROCK-II. While this data confirmed that ROCK-II localized to invadopodia, it did not

necessary prove that it was a critical mediator of colon cancer cell invasion.

### ROCK-II Mediates Colon Cancer Cell Invasion

To verify that ROCK-II mediated invasion via invadopodia in colon cancer cell lines, we next evaluated the effect of knocking down ROCK-II with siRNA on depth of invasion and actin cytoskeletal morphology. All siRNA experiments were performed with a scrambled sequence siCONTROL, which did not significantly reduce ROCK-II expression, depth of invasion, proliferation, or MMP activity. Transfection efficiency of ROCK-II siRNA in all cell lines was between 60 and 90%. A representative western blot of SW620 lysates is shown in Figure 5f.

When we evaluated the depth of invasion following ROCK-II knockdown, there was no significant decrease in the depth of invasion by either non-malignant intestinal cell line (data not shown). There was a slight, but not significant decrease in invasion in Caco-2 E cells in which ROCK-II had been silenced (data not shown). However, ROCK-II knockdown did produce greater than three-fold decrease in the

depth of invasion by HCT-116 cells and nearly a two-fold decrease in the depth of invasion by SW620 cells (Figure 5e).

In addition to the invasion depth, cell morphology was altered due to ROCK-II knockdown. The most dramatic effect was seen in SW620 cells (Figure 5a–d). Specifically, untransfected SW620 cells have an elongated appearance with protrusions coming from the main cell body and stained brightly with phalloidin, which preferentially binds at the interface of F-actin subunits (Figure 5a and c). However, cells in which ROCK-II had been knocked down had significantly fewer phalloidin-staining protrusions and a weak actin signal, compatible with successful knockdown of ROCK-II

whose activity is important to the formation of F-actin (Figure 5b and d).

### ROCK-II Does Not Mediate Proliferation in Colon Cancer Cells

It could be said that less invasion occurred because siRNA inhibition of ROCK-II impaired cell proliferation. When we evaluated proliferation in each of the three colon cancer cell lines as well as both non-malignant intestinal cell lines at 24 h post invasion without and with ROCK-II knockdown, no significant change in proliferation was seen in any of the three colon cancer cell lines in which ROCK-II had been

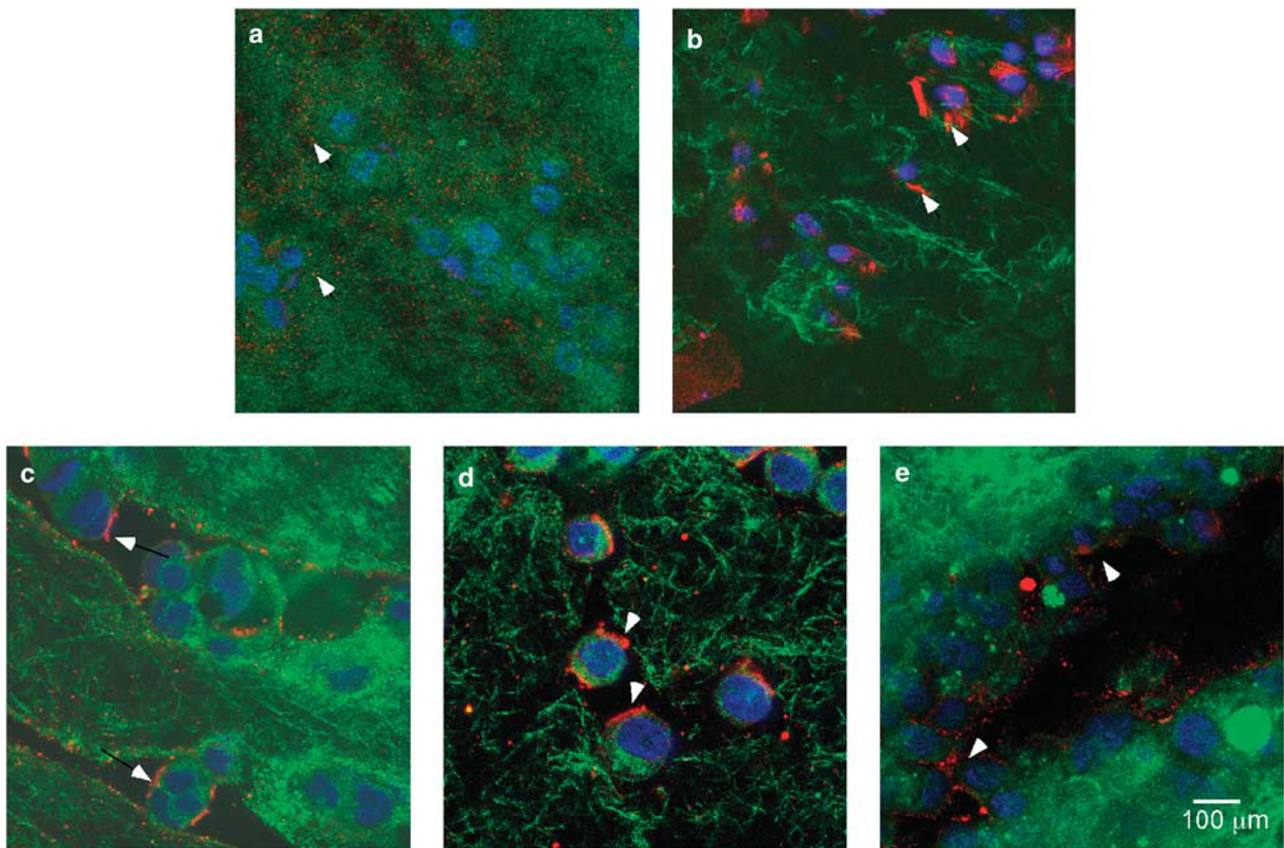
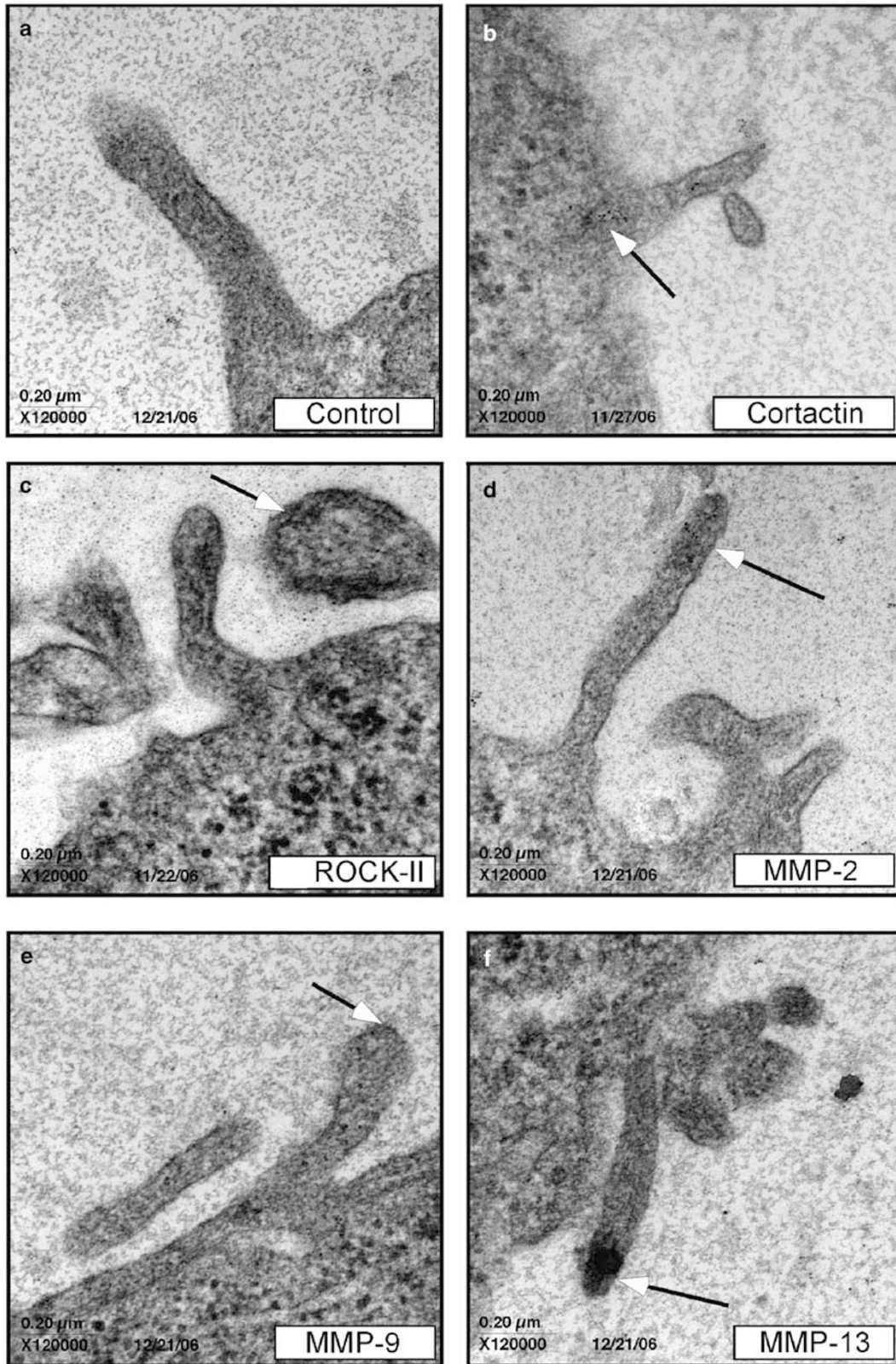


**Figure 3** ROCK-II collections are directly associated with areas of collagen degradation in colon cancer cell-containing scaffolds but not in scaffolds containing non-malignant intestinal cell types. Non-malignant (NCM 460 (a) and IEC-6 (b)) and malignant intestinal cell lines (Caco-2 E (c), SW620 (d), and HCT-116 (e)) were seeded onto type I collagen scaffolds and allowed to invade over a 24-h period. Cell-containing scaffolds were then fixed, probed for ROCK-II (red), and nuclei were stained with DAPI (blue). Collagen autofluorescence is shown in green. Similar to data shown in Figure 2, ROCK-II is expressed at the cell periphery in each of the three colon cancer cell lines (c–e) evaluated but the collagen adjacent to these structures is clearly absent. This finding was not observed in either non-malignant intestinal cell line ((a) NCM460 and (b) IEC-6). Negative controls for each cell line were probed with a goat IgG and no staining was seen (data not shown). Bar = 100  $\mu$ m.

**Figure 4** TEM images reveal that ROCK-II, MMP-2, and MMP-13 localize to invadopodia in colon cancer cell lines. All cell lines were allowed to invade 1.5 mg/ml type I collagen scaffolds over a 24-h period. Scaffolds were then fixed and embedded in epoxy resin. Representative images of SW620 cells stained with a goat IgG (a), and antibodies to cortactin (b), ROCK II (c), MMP-2 (d), MMP-9 (e), or MMP-13 (f) followed by appropriate secondary antibody conjugated to 6 nm gold particles and counterstaining are shown. Intense areas of black indicate the presence of antigen being probed and are indicated by arrows. ROCK-II, MMP-2, and MMP-13 (c, d, and f) localized to the tips of invadopodia. Minimal MMP-9 staining was present (e). Cortactin staining was noted at the base of the invadopodia (b). Extracellular material is type I collagen. Invadopodia were also seen on TEM in Caco-2 E and HCT-116 cells but were not seen in either non-malignant intestinal cell type (data not shown) Bar = 0.2  $\mu$ m.

silenced. However, ROCK-II knockdown produced a nearly two-fold decrease in proliferation in both non-malignant intestinal cell lines (Figure 6). This was an important finding

since ROCK-II has previously been linked with apoptosis<sup>19,33</sup> but not proliferation. In addition, these data suggest for the first time that ROCK-II may act as a regulator of proliferation



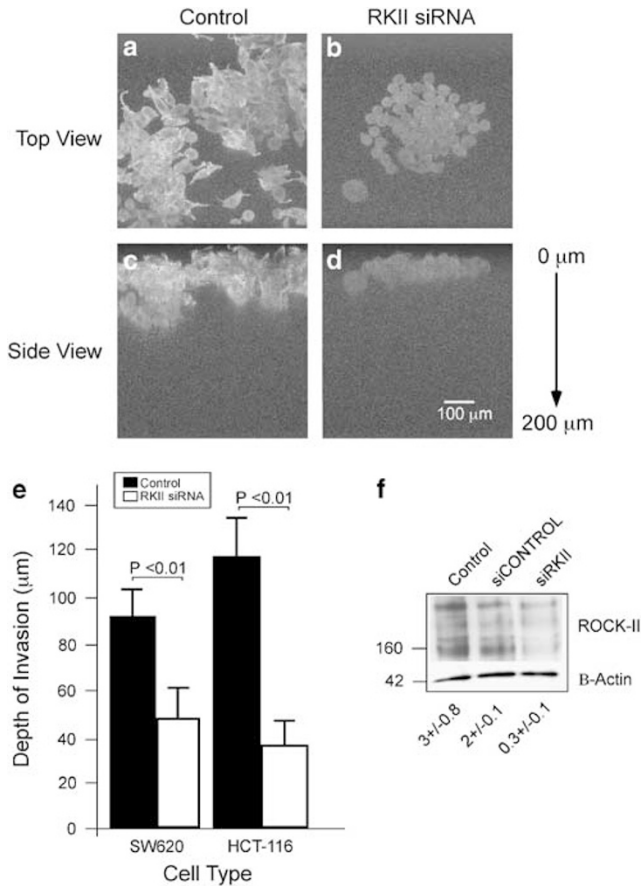


**Figure 5** ROCK-II modulates colon cancer cell invasion. All cell lines were allowed to invade type I collagen scaffolds 48 h after transfection with ROCK-II siRNA. Representative multiphoton images of untransfected and transfected SW60 cells following staining with phalloidin are shown in (a–d). Panels a and b are top views, whereas panels c and d are 200-µm-thick digital reconstructions of images taken every 1 µm. As shown in (a and c), untreated SW620 cells were more elongated, had more projections, and had more intense actin staining. In contrast, SW620 cells treated with ROCK-II siRNA were more rounded, had few projections, invaded less, and had less intense actin staining (b and d). Bar = 100 µm. Quantitative analysis of the depth of invasion is shown in (e). The most significant effects ( $P < 0.01$ ) of ROCK-II silencing were seen in the two most tumorigenic colon cancer cell lines; SW620 and HCT-116. Control samples are in black and ROCK-II knockdown samples are in white. Transfection with siCONTROL did not lead to a significant change in the depth of invasion (data not shown). A representative western blot showing ROCK-II expression in extracts from untransfected SW620 cells and SW620 cells transfected with siCONTROL or ROCK-II siRNA is shown in (f). Densitometry data are recorded below each lane.

during normal tissue turnover in the intestine, but becomes a broker of invasion in the setting of colon cancer.

**ROCK-II Influences MMP Activity**

In Figure 4 above, we show for the first time that ROCK-II localizes to invadopodia in colon cancer cells along with MMP-2, MMP-13, and to a significantly lesser extent, MMP-9. Furthermore, we show that knock down of ROCK-II impairs colon cancer invasion but not colon cancer proliferation. Based on these data, we hypothesized that ROCK-II was

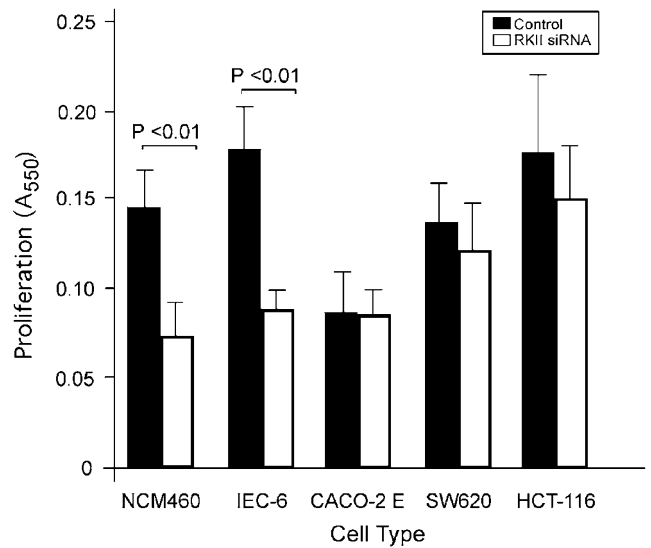


**Figure 6** ROCK-II modulates proliferation in non-malignant intestinal cells, but not colon cancer cells. Proliferation was determined using an MTT assay as described in the Materials and methods section. ROCK-II knockdown produced a more than two-fold decrease ( $P < 0.05$ ) in proliferation in both non-malignant intestinal cell lines (NCM460 and IEC-6), but produced no significant change in proliferation in any of the colon cancer cell lines (Caco-2 E, SW620, and HCT-116). Control samples are in black and ROCK-II knockdown samples are in white.

modulating a critical checkpoint in colon cancer cell invasion through its action on MMPs at the site of invadopodia. To test this, we evaluated MMP-2, -9, and -13 activities using commercially available sandwich ELISA kits. This particular assay has been validated against zymography, and therefore served as a high-throughput method for observing changes in MMP activity.

As shown in Figure 7, overall MMP activity was higher in all the three colon cancer cell lines as compared with both non-malignant intestinal cell types. Knock down of ROCK-II led to significant reduction ( $P < 0.05$ ) in both MMP-2 and MMP-13 in all the three colon cancer cell lines, but not in non-malignant NCM460 cells. In IEC-6 cells, ROCK-II knockdown led to a significant increase in MMP-9 and a significant increase in MMP-2. We do not know the reason for this but hypothesize that ROCK-II may serve as important regulator of these MMPs in the small intestine. It may also be that MMP-2 activity is modulated by ROCK-II in the small intestine but not in the colon. Taken together, these data suggest that ROCK-II acts as an important regulator of both invasion and regulated MMP-2 and -13 release at the site of invadopodia.

**DISCUSSION**

Colon cancer remains the second leading cause of cancer death in the United States and the third leading cause of cancer death globally because of limitations related to the treatment of advanced disease. ROCK has been felt to be a possible target in this battle against metastatic disease, but its

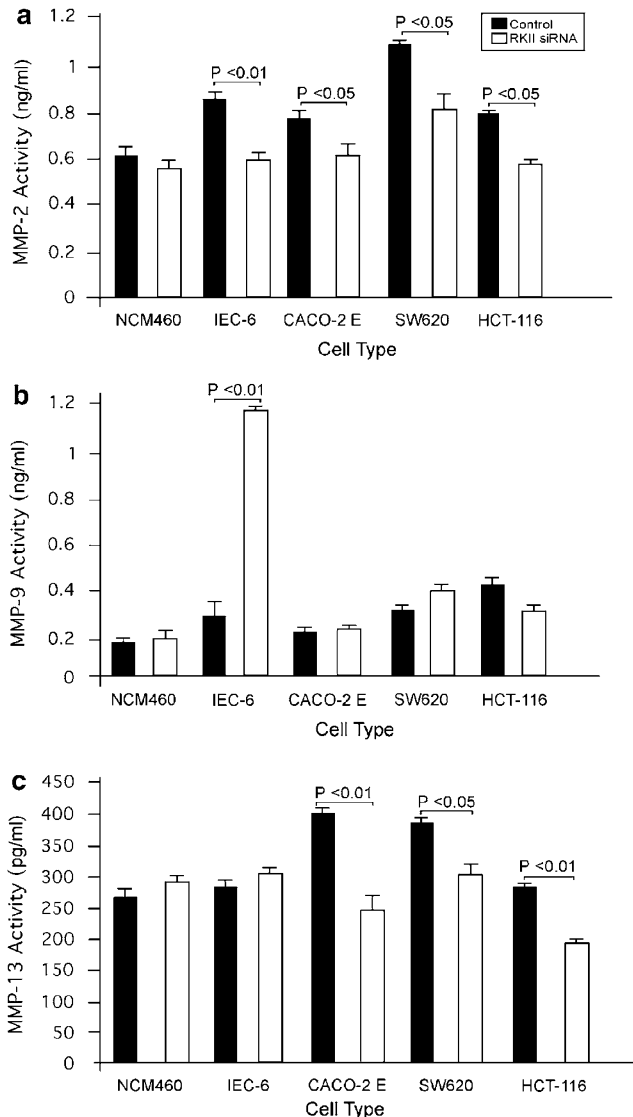


**Figure 7** ROCK-II modulates MMP-2 and -13 activities. MMP-2 (a), MMP-9 (b), and MMP-13 (c) activities were determined using a commercially available ELISA sandwich assay as described in the Materials and methods section. ROCK-II knockdown led to significant decreases in MMP-2 and -13 activities in all colon cancer cell lines (Caco-2 E, SW620, and HCT-116). IEC-6 showed a significant decrease in MMP-2 and a significant increase in MMP-9 due to ROCK-II knockdown. MMP activity in NCM460 cells was not significantly affected by ROCK-II knockdown. An increase in MMP-13 expression has been previously linked to a poor outcome in colon cancer. Control samples are in black and ROCK-II knockdown samples are in white.

role in invasion has not been well understood. Because ROCK-II has been linked with greater invasion and metastasis in several solid tumors, we evaluated ROCK-II's contribution to colon cancer cell invasion in dense type I collagen scaffolds—an environment more reminiscent of the advancing edge of a colon cancer. Using this model, we demonstrated for the first time that ROCK-II contributes to colon cancer cell invasion through its action on MMP-2 and -13 at the site of invadopodia.

Our data confirm the finding by others that ROCK is involved in the activation of matrix metalloproteases, specifically MMP-2, MMP-9, and MMP-13.<sup>34,35</sup> Furthermore, it identifies ROCK-II as the critical isoform of ROCK involved in activation of both MMP-2 and MMP-13. MMP-9 activity has also been linked to Rho/ROCK,<sup>36</sup> but our data did not show a significant decrease in MMP-9 activity with ROCK-II knockdown. The reason for this is not clear but what is clear is that there is regulation of MMPs by ROCK-II in the setting of an *in vitro* colon cancer model. Furthermore, the link between MMP-13 and ROCK-II in colon cancer confirms the retrospective studies that associated MMP-13 with a poor prognosis in colon cancer<sup>37,38</sup> as well as the studies showing that inhibition of ROCK not MMPs attenuates invasion.<sup>39</sup>

The finding of ROCK-II colocalizing with invadopodia was not expected particularly in light of the recent literature showing ROCK to be a mediator of amoeboid cell movement.<sup>39–41</sup> Mesenchymal cell movement is associated with matrix degradation, whereas amoeboid cell movement relies on the cell's ability to use the force of actomyosin to push collagen fibers out of the way. A study by Sahai *et al* reported that mesenchymal invasion by breast cancer, colon cancer, melanoma, and fibrosarcoma cell lines is mediated by Smurf1 promotion of Rho A degradation and subsequent decrease in ROCK activity. Furthermore, this group reported that when Smurf1 is inhibited, invasion increases and cell movement becomes more amoeboid—processes which they linked to increased ROCK activity. Intriguingly, the inhibitors used in this study targeted ROCK-I (Y-27632)<sup>42</sup> and did not target MMP-13.<sup>39,40</sup> Similarly, two other groups have linked ROCK with amoeboid cell movement. A study by Wyckoff *et al* reported that ROCK-I and -II contribute to amoeboid cell movement. In this study, a highly invasive breast cancer cell line, MTLn3E, was studied in 4 mg/ml type I collagen gels. One could argue at this density that mesenchymal cell movement was not necessary because of the increase in porosity of the gel created by tight packing of collagen fibers.<sup>39,40</sup> A third paper by Torika *et al* reported that inhibition of ROCK with Y-27632 in aggressive breast cancer cells grown in 1.67 mg/ml type I collagen scaffolds led these cells to change from an amoeboid to a mesenchymal appearance.<sup>39,40</sup> We would argue that this is due to an increase in ROCK-II activity and that the ROCK activities they report were obtained from cells grown on tissue culture plastic, not from cells grown in type I collagen scaffolds. Taken together, these studies confirm that ROCK-II may have different activities depending on chemical and mechanical signals of the local microenvironment.<sup>43</sup> In addition, they emphasize the importance of the tumor microenvironment to understanding and predicting tumor cell invasion. In the case of colon cancer invasion, our *in vitro* model shows that a colon cancer cell's ability to invade at the tumor advancing edge is mediated, in large part, by the action of ROCK-II on MMP-2 and -13 at the site of invadopodia. In conclusion, our data

suggest that ROCK-II as a potential target for attenuating colon cancer cell invasion.

#### ACKNOWLEDGEMENT

We thank Dr Kenneth Wilson for his patience and faithful reminders that we need to get our papers out. We also thank Dr Alissa Weaver for her insight and advice regarding invadopodia, and Linda Juarez in the UIC EM facility for her advice and excellent work on our TEM images. The Elisa Pardee Foundation supported this work.

- Kamai T, Tsujii T, Arai K, *et al*. Significant association of Rho/ROCK pathway with invasion and metastasis of bladder cancer. *Clin Cancer Res* 2003;9:2632–2641.
- Horiuchi A, Imai T, Wang C, *et al*. Up-regulation of small GTPases, RhoA and RhoC, is associated with tumor progression in ovarian carcinoma. *Lab Invest* 2003;83:861–870.
- Huq J, Elgohary B, Guzman G, *et al*. Rho-like proteins in human colon cancers are uniquely expressed as a function of differentiation and tumor invasion. *Gastroenterology* 2006;130:A679.
- Kuphal S, Palm HG, Poser I, *et al*. Snail-regulated genes in malignant melanoma. *Melanoma Res* 2005;15:305–313.
- Han G, Lu SL, Li AG, *et al*. Distinct mechanisms of TGF-beta1-mediated epithelial-to-mesenchymal transition and metastasis during skin carcinogenesis. *J Clin Invest* 2005;115:1714–1723.
- Nakahara H, Mueller SC, Nomizu M, *et al*. Activation of beta1 integrin signaling stimulates tyrosine phosphorylation of p190RhoGAP and membrane-protrusive activities at invadopodia. *J Biol Chem* 1998;273:9–12.
- Bellovin DI, Bates RC, Muzikansky A, *et al*. Altered localization of p120 catenin during epithelial to mesenchymal transition of colon carcinoma is prognostic for aggressive disease. *Cancer Res* 2005;65:10938–10945.
- Ozdamar B, Bose R, Barrios-Rodiles M, *et al*. Regulation of the polarity protein Par6 by TGFbeta receptors controls epithelial cell plasticity. *Science* 2005;307:1603–1609.
- Sahai E, Marshall CJ. ROCK and Dia have opposing effects on adherens junctions downstream of Rho. *Nat Cell Biol* 2002;4:408–415.
- Croft DR, Sahai E, Mavria G, *et al*. Conditional ROCK activation *in vivo* induces tumor cell dissemination and angiogenesis. *Cancer Res* 2004;64:8994–9001.
- Bosman FT. Prognostic value of pathological characteristics of colorectal cancer. *Eur J Cancer* 1995;31A:1216–1221.
- Hase K, Shatney C, Johnson D, *et al*. Prognostic value of tumor 'budding' in patients with colorectal cancer. *Dis Colon Rectum* 1993;36:627–635.
- Wood CB, Gillis CR, Hole D, *et al*. Local tumor invasion as a prognostic factor in colorectal cancer. *Br J Surg* 1981;68:326–328.
- Pyke C, Salo S, Ralfkiaer E, *et al*. Laminin-5 is a marker of invading cancer cells in some human carcinomas and is coexpressed with the receptor for urokinase plasminogen activator in budding cancer cells in colon adenocarcinomas. *Cancer Res* 1995;55:4132–4139.
- Sun S, Wise J, Cho M. Human fibroblast migration in three-dimensional collagen gel in response to noninvasive electrical stimulus. I. Characterization of induced three-dimensional cell movement. *Tissue Eng* 2004;10:1548–1557.
- Moyer MP, Stauffer J, Manzano L, *et al*. NCM460, a normal human colon mucosal epithelial cell line. *In Vitro Cell Devel Biol (Animal)* 1996;32:315–317.
- Leibovitz A, Stinson JC, McCombs III WB, *et al*. Classification of human colorectal adenocarcinoma cell lines. *Cancer Res* 1976;36:4562–4569.
- Flatmark K, Maelandsmo GM, Martinsen M, *et al*. Twelve colorectal cancer cell lines exhibit highly variable growth and metastatic capacities in an orthotopic model in nude mice. *Eur J Cancer* 2004;40:1593–1598.
- Sebbagh M, Hamelin J, Bertoglio J, *et al*. Direct cleavage of ROCK II by granzyme B induces target cell membrane blebbing in a caspase-independent manner. *J Exp Med* 2005;201:465–471.
- Marx J. Cell biology. Podosomes and invadopodia help mobile cells step lively. *Science* 2006;312:1868–1869.
- Buccione R, Orth JD, McNiven MA. Foot and mouth: podosomes, invadopodia and circular dorsal ruffles. *Nat Rev Mol Cell Biol* 2004;5:647–657.
- Nagi C, Bleiweiss IJ. Invadopodia and cancer cell migration. *Adv Anat Pathol* 2007;14:55–56.
- Yamaguchi H, Pixley F, Condeelis J. Invadopodia and podosomes in tumor invasion. *Eur J Cell Biol* 2006;85:213–218.
- Weaver AM. Invadopodia: specialized cell structures for cancer invasion. *Clin Exp Metastasis* 2006;23:97–105.
- Bowden ET, Onikoyi E, Slack R *et al*. Co-localization of cortactin and phosphotyrosine identifies active invadopodia in human breast cancer cells. *Exp Cell Res* 2006;312:1240–1253.
- Artym VV, Zhang Y, Seillier-Moisewitsch F, *et al*. Dynamic interactions of cortactin and membrane type 1 matrix metalloproteinase at invadopodia: defining the stages of invadopodia formation and function. *Cancer Res* 2006;66:3034–3043.
- Bowden ET, Barth M, Thomas D, *et al*. An invasion-related complex of cortactin, paxillin and PKCmu associates with invadopodia at sites of extracellular matrix degradation. *Oncogene* 1999;18:4440–4449.
- Nagase H. Cell surface activation of progelatinase A (proMMP-2) and cell migration. *Cell Res* 1998;8:179–186.
- Deryugina EI, Ratnikov B, Monosov E, *et al*. MT1-MMP initiates activation of pro-MMP-2 and integrin alphavbeta3 promotes maturation of MMP-2 in breast carcinoma cells. *Exp Cell Res* 2001;263:209–223.
- Coopman PJ, Do MT, Thompson EW, *et al*. Phagocytosis of cross-linked gelatin matrix by human breast carcinoma cells correlates with their invasive capacity. *Clin Cancer Res* 1998;4:507–515.
- Bourguignon LY, Gunja-Smith Z, Iida N, *et al*. CD44v(3,8–10) is involved in cytoskeleton-mediated tumor cell migration and matrix metalloproteinase (MMP-9) association in metastatic breast cancer cells. *J Cell Physiol* 1998;176:206–215.
- Elnemr A, Yonemura Y, Bandou E, *et al*. Expression of collagenase-3 (matrix metalloproteinase-13) in human gastric cancer. *Gastric Cancer* 2003;6:30–38.
- Orlando KA, Pittman RN. Rho kinase regulates phagocytosis, surface expression of GlcNAc, and Golgi fragmentation of apoptotic PC12 cells. *Exp Cell Res* 2006;312:3298–3311.
- Meriane M, Duhamel S, Lejeune L, *et al*. Cooperation of matrix metalloproteinases with the RhoA/Rho kinase and mitogen-activated protein kinase kinase-1/extracellular signal-regulated kinase signaling pathways is required for the sphingosine-1-phosphate-induced mobilization of marrow-derived stromal cells. *Stem Cells* 2006;24:2557–2565.
- Fukushima M, Nakamura M, Kohjima M, *et al*. Fasudil hydrochloride hydrate, a Rho-kinase (ROCK) inhibitor, suppresses collagen production and enhances collagenase activity in hepatic stellate cells. *Liver Int* 2005;25:829–838.
- Turner NA, O'Regan DJ, Ball SG, *et al*. Simvastatin inhibits MMP-9 secretion from human saphenous vein smooth muscle cells by inhibiting the RhoA/ROCK pathway and reducing MMP-9 mRNA levels. *FASEB J* 2005;19:804–806.
- Klinge U, Rosch R, Junge K, *et al*. Different matrix micro-environments in colon cancer and diverticular disease. *Int J Colorectal Dis* 2006;22:515–520.
- Leeman MF, McKay JA, Murray GI. Matrix metalloproteinase 13 activity is associated with poor prognosis in colorectal cancer. *J Clin Pathol* 2002;55:758–762.
- Wyckoff JB, Pinner SE, Gschmeissner S, *et al*. ROCK- and myosin-dependent matrix deformation enables protease-independent tumor-cell invasion *in vivo*. *Curr Biol* 2006;16:1515–1523.
- Torka R, Thuma F, Herzog V, *et al*. ROCK signaling mediates the adoption of different modes of migration and invasion in human mammary epithelial tumor cells. *Exp Cell Res* 2006;312:3857–3871.
- Sahai E, Garcia-Medina R, Pouyssegur J, *et al*. Smurf1 regulates tumor cell plasticity and motility through degradation of RhoA leading to localized inhibition of contractility. *J Cell Biol* 2007;176:35–42.
- Tamura M, Nakao H, Yoshizaki H, *et al*. Development of specific Rho-kinase inhibitors and their clinical application. *Biochim Biophys Acta* 2005;1754:245–252.
- Wozniak MA, Desai R, Solski PA, *et al*. ROCK-generated contractility regulates breast epithelial cell differentiation in response to the physical properties of a three-dimensional collagen matrix. *J Cell Biol* 2003;163:583–595.